

# LOW-COMPLEXITY RECONSTRUCTION OF SAMPLED GRAPH SIGNALS IN LOCAL GRAPH FOURIER SUBSPACES

Gerald Matz

*Institute of Telecommunications, TU Wien*  
 Email: gerald.matz@tuwien.ac.at

**Abstract**—In our prior work, we have introduced local graph Fourier frames (LGFFs) as a flexible and powerful modeling and analysis tool for graph signals. The most important practical advantage of LGFFs is their outstanding computational efficiency. In this paper, we discuss the vertex-domain sampling and interpolation (recovery) of graph signals that live in an LGFF subspace. We formulate perfect reconstruction conditions and develop low-complexity recovery algorithms that also work in the presence of measurement noise. Furthermore, we discuss interesting special cases and illustrate our framework by numerical experiments.

## I. INTRODUCTION

Graph signal processing (GSP) by now has become a highly active and practically relevant field in signal processing [1–3]. Its goal is to extend conventional signal processing concepts to data on irregular domains characterized by combinatorial graphs. While there has been huge progress with regard to the theoretical understanding of GSP, the practical application of many ideas to large real-world graphs is hampered by a huge computational burden, most importantly due to the fact that the graph Fourier transform (GFT) in general does not admit an efficient implementation.

A topic that has received a lot of interest in the GSP community is the sampling and reconstruction of graph signals (see [4] for a recent overview), where there have been essentially two approaches. The first approach is model-based and assumes that the graph signal has a sparse representation in terms of the GFT or in terms of a graph filter [5–11]; this approach bears similarities to classical sampling theory and enables the analysis and design of suitable sampling sets but in general suffers from high complexity. The second approach is model-free and attempts signal reconstruction by enforcing smoothness constraints on the graph signal [12–14]; this approach often results in computationally attractive reconstruction algorithms but is not easily accessible to theoretical analysis. In this paper, we introduce a sampling and interpolation framework that combines the advantages of these two approaches by building on the notion of local graph Fourier frames (LGFFs). We introduced LGFFs in our recent work [15] as a computationally extremely attractive workhorse for graph signal analysis and processing that builds on graph partitions and is preferable to spectral graph wavelets [16] and spectrally localized graph frames [17–20]. The GFT and the methods in [21, 22] can be viewed as simple special cases of our LGFF framework.

Here, we formulate an LGFF-based signal model that amounts to a local bandlimitation and we discuss vertex-domain sampling and interpolation of such signals. We study

conditions for perfect signal recovery, develop suitable signal reconstruction algorithms, analyze special cases, and demonstrate the performance of our method in terms of numerical simulations. Our findings corroborate that our approach has excellent performance despite very low computational complexity. Furthermore, even if perfect reconstruction fails, the interpolation errors typically remain localized to a small subset of vertices, a property that is highly attractive from a practical perspective.

Our paper is organized as follows. In Section II, we review the definition and design of LGFFs and introduce our LGFF subspace signal model. In Section III we formulate the sampling and reconstruction problem, develop our reconstruction method, and discuss computational aspects and special cases. In Section IV we illustrate our findings with numerical simulations. Conclusions are provided in Section V.

## II. LOCAL GRAPH FOURIER FRAMES AND SUBSPACES

### A. LGFF

Consider an undirected graph  $\mathcal{G}$  with vertex set  $\mathcal{V} = \{1, \dots, N\}$  and weighted adjacency matrix  $\mathbf{W} \in \mathbb{R}^{N \times N}$ . We denote by  $\mathbf{g}_k = (g_k[1], \dots, g_k[N])^T$ ,  $k = 1, \dots, K$ , a collection of window functions on  $\mathcal{G}$ . The vertex support of  $\mathbf{g}_k$  is defined as

$$\mathcal{S}_k \triangleq \{n: |g_k[n]| > 0\}.$$

The sets  $\mathcal{S}_k$  and hence the window functions  $\mathbf{g}_k$  may overlap. Denote by  $\mathcal{G}_k$  the subgraph induced by  $\mathcal{S}_k$  (assumed to be connected) and let  $\mathbf{W}_k \in \mathbb{R}^{N_k \times N_k}$  its weighted adjacency matrix, with  $N_k \triangleq |\mathcal{S}_k|$  the number of nodes in  $\mathcal{G}_k$ . The (local) graph Fourier basis for  $\mathcal{G}_k$  is given by the (orthonormal) eigenvectors  $\mathbf{u}_{kl}$ ,  $l = 1, \dots, N_k$ , of the Laplacian  $\mathbf{L}_k = \text{Diag}(\mathbf{W}_k \mathbf{1}) - \mathbf{W}_k$  [1, 2]. (Here,  $\text{Diag}(\mathbf{d})$  denotes a diagonal matrix whose main diagonal is given by  $\mathbf{d}$ .) We assume that the eigenvectors are sorted according to increasing eigenvalues; the first eigenvector equals 0 and the associated eigenvector is constant,  $\mathbf{u}_{k1} = \mathbf{1}/\sqrt{N_k}$ . The windowed local graph Fourier basis vectors are then defined by [15]

$$\mathbf{f}_{kl} \triangleq \mathbf{g}_k \odot \mathbf{S}_k \mathbf{u}_{kl}, \quad k = 1, \dots, K, \quad l = 1, \dots, N_k,$$

where  $\odot$  denotes the element-wise vector product. Here, the matrix  $\mathbf{S}_k \in \{0, 1\}^{N \times N_k}$  zero-pads the length- $N_k$  eigenvectors  $\mathbf{u}_{kl}$  to length- $N$  signals on the full graph  $\mathcal{G}$ . Equivalently, we can express the basis vectors in terms of their elements as  $f_{kl}[n] = g_k[n]u_{kl}[n]$ , with  $u_{kl}[n]$  being the zero-padded

versions of the eigenfunctions  $\mathbf{u}_{kl}$ . We arrange the vectors  $\mathbf{f}_{kl}$ ,  $k = 1, \dots, K$ ,  $l = 1, \dots, N_k$ , into the matrix

$$\mathbf{F} = (\mathbf{f}_{11}, \dots, \mathbf{f}_{1N_1}, \mathbf{f}_{21}, \dots, \mathbf{f}_{2N_2}, \dots, \mathbf{f}_{K1} \dots \mathbf{f}_{KN_K}).$$

This matrix has  $N$  rows and  $N' \triangleq \sum_{k=1}^K N_k$  columns.

In [15] we have shown that  $\mathbf{F}$  is a Parseval frame [23] (i.e.,  $\mathbf{F}\mathbf{F}^T = \mathbf{I}$ ) if and only if the window functions  $\mathbf{g}_k$  satisfy

$$\sum_{k=1}^K \mathbf{g}_k \odot \mathbf{g}_k = \mathbf{1}, \quad (1)$$

equivalently,  $\sum_{k=1}^K g_k^2[n] = 1$ . This condition requires that  $N' \geq N$ . The case  $N' = N$  necessitates constant windows with disjoint support and reobtains the bases from [21, 22] as special cases. We refer to  $\mathbf{F}$  as *local graph Fourier frame* (LGFF) since its construction resembles local Fourier bases [24] and lapped orthogonal transforms [25].

We next recall the window design from [15]. Let  $\mathcal{V}_1, \dots, \mathcal{V}_K$  denote a partition of the vertex set into disjoint subsets, i.e.,  $\mathcal{V} = \bigcup_{k=1}^K \mathcal{V}_k$ ,  $\mathcal{V}_k \cap \mathcal{V}_{k'} = \emptyset$  for  $k \neq k'$ . The indicator function of  $\mathcal{V}_k$  is denoted by  $\chi_k$ . By definition, we have  $\sum_{k=1}^K \chi_k = \mathbf{1}$ . Next, consider a graph filter  $\mathbf{G}$  with nonnegative filter coefficients that satisfies  $\mathbf{G}\mathbf{1} = \mathbf{1}$ . Then, the windows  $\mathbf{g}_k$  defined by  $\mathbf{g}_k \odot \mathbf{g}_k = \mathbf{G}\chi_k$  satisfy (1) and therefore induce a Parseval LGFF. An attractive choice for  $\mathbf{G}$  amounts to polynomials of the random walk weighted adjacency matrix  $\widetilde{\mathbf{W}} = \text{Diag}^{-1}(\mathbf{W}\mathbf{1})\mathbf{W}$ ,

$$\mathbf{G} = \sum_{i=0}^I \eta_i \widetilde{\mathbf{W}}^i.$$

Here, the filter coefficients  $\eta_i \geq 0$  are normalized as  $\sum_{i=0}^I \eta_i = 1$ . With this construction, the windows  $\mathbf{g}_k$  have a smooth roll-off and a support  $\mathcal{S}_k$  that equals the  $I$ -hop neighborhood of  $\mathcal{V}_k$ .

### B. Signal Model

Our LGFF constitute an (over)complete basis in  $\mathbb{R}^N$ . For sampling and interpolation we are interested in classes of sufficiently smooth graph signals. Hence, we are imposing a local lowpass constraint, i.e., we assume that within each subgraph  $\mathcal{G}_k$  only the first few LGFF vectors (with small  $l$ ) are relevant. More specifically, our signal model comprises only LGFF vectors with  $l \leq B_0 \ll N_k$ ,

$$\mathbf{s} = \sum_{k=1}^K \sum_{l=1}^{B_0} \xi_{kl} \mathbf{f}_{kl} = \overline{\mathbf{F}}\boldsymbol{\xi}. \quad (2)$$

Here, the basis matrix and coefficient vector are defined as

$$\begin{aligned} \overline{\mathbf{F}} &= (\mathbf{f}_{11}, \dots, \mathbf{f}_{1B_0}, \dots, \mathbf{f}_{K1} \dots \mathbf{f}_{KB_0}) \in \mathbb{R}^{N \times B}, \\ \boldsymbol{\xi} &= (\xi_{11}, \dots, \xi_{1B_0}, \dots, \xi_{K1}, \dots, \xi_{KB_0}) \in \mathbb{R}^B, \end{aligned}$$

with  $B = KB_0$  denoting the total degrees of freedom. The complexity of synthesizing  $\mathbf{s}$  from the coefficients  $\xi_{kl}$  scales as  $\mathcal{O}(\eta NB/K)$  and hence is essentially linear in the signal length  $N$ . We refer to the set of signals consistent with (2) as a local graph Fourier subspace (LGFS). The extension to

distinct ‘‘local bandwidths’’ within each subgraph is trivial; nonetheless, for simplicity we here restrict ourselves to the same local bandwidth  $B_0$  for all  $k$ .

For the special case  $B_0 = 1$ , we have  $\mathbf{f}_{k1} = \frac{1}{\sqrt{N_k}}\mathbf{g}_k$  since  $\mathbf{u}_{k1} = \mathbf{1}/\sqrt{N_k}$ , and hence we obtain an LGFS with  $B = K$  dimensions that amounts to

$$\mathbf{s} = \sum_{k=1}^K \frac{1}{\sqrt{N_k}} \xi_k \mathbf{g}_k;$$

furthermore,  $\overline{\mathbf{F}} = (\mathbf{g}_1 \dots \mathbf{g}_K) \text{Diag}(\sqrt{1/N_1} \dots \sqrt{1/N_K})$ . If in addition the windows are non-overlapping (and hence constant,  $\mathbf{g}_k = \mathbf{1}$ ), the basis  $\overline{\mathbf{F}}$  becomes orthonormal and models graph signals that are piecewise constant.

## III. SAMPLING AND RECONSTRUCTION

### A. Proposed Method

We consider simple vertex-domain sampling of a (possibly noisy) LGFS signal  $\mathbf{s}$ . Let  $\mathcal{M} = \{n_1, \dots, n_M\} \subseteq \mathcal{V}$  denote the sampling set of cardinality  $M$  and define the associated sampling matrix as  $\mathbf{M} = (\mathbf{e}_{n_1} \dots \mathbf{e}_{n_M})^T \in \{0, 1\}^{M \times N}$ . The sampled LGFS signal is then given by

$$\mathbf{x} = \mathbf{M}\mathbf{s} + \mathbf{v},$$

where  $\mathbf{v}$  denotes measurement noise. We define the oversampling ratio as  $\eta = M/B$ . Our goal is to design a linear reconstruction scheme for the signal  $\mathbf{s}$ ,

$$\hat{\mathbf{s}} = \mathbf{A}\mathbf{x},$$

such that the reconstructed signal obeys the signal model (2), i.e.,  $\hat{\mathbf{s}} \in \text{span}\{\overline{\mathbf{F}}\}$ , equivalently  $\hat{\mathbf{s}} = \overline{\mathbf{F}}\hat{\boldsymbol{\xi}}$ . If there is no noise, we can aim for perfect reconstruction, i.e.,  $\hat{\mathbf{s}} = \mathbf{s}$  or equivalently  $\hat{\mathbf{s}} = \overline{\mathbf{F}}\hat{\boldsymbol{\xi}}$  with  $\hat{\boldsymbol{\xi}} = \mathbf{A}'\mathbf{x} = \boldsymbol{\xi}$ . Since in the noise-free case  $\mathbf{x} = \mathbf{M}\mathbf{s} = \mathbf{M}\overline{\mathbf{F}}\boldsymbol{\xi}$ , we arrive at the condition

$$\mathbf{A}'\overline{\mathbf{F}}\boldsymbol{\xi} = \boldsymbol{\xi}, \quad (3)$$

where we defined the  $M \times B$  sampled basis matrix  $\widetilde{\mathbf{F}} = \mathbf{M}\overline{\mathbf{F}}$ , whose columns are the sampled LGFF vectors. Condition (3) says that  $\mathbf{A}'$  must be a left-inverse of  $\widetilde{\mathbf{F}}$ . This in turn requires that the columns of  $\widetilde{\mathbf{F}}$  are linearly independent, for which  $M \geq B$  (i.e.,  $\eta \geq 1$ ) is a necessary condition. A solution for  $\mathbf{A}'$  is given by Moore-Penrose pseudo-inverse  $\widetilde{\mathbf{F}}^\#$  of  $\widetilde{\mathbf{F}}$  and hence

$$\hat{\mathbf{s}} = \overline{\mathbf{F}}\hat{\boldsymbol{\xi}}, \quad \hat{\boldsymbol{\xi}} = \widetilde{\mathbf{F}}^\#\mathbf{x}. \quad (4)$$

When  $\widetilde{\mathbf{F}}$  has full rank, the Moore-Penrose pseudo-inverse can be written as

$$\widetilde{\mathbf{F}}^\# = (\widetilde{\mathbf{F}}^T\widetilde{\mathbf{F}})^{-1}\widetilde{\mathbf{F}}^T$$

and we have perfect reconstruction in the noise-free case where  $\mathbf{x} = \widetilde{\mathbf{F}}\boldsymbol{\xi}$ , i.e.,  $\hat{\boldsymbol{\xi}} = \boldsymbol{\xi}$  and  $\hat{\mathbf{s}} = \mathbf{s}$ . If the samples are affected by i.i.d. noise with variance  $\sigma^2$ , the mean-square reconstruction error achieved by (4) can be shown to equal

$$\mathbb{E}\{\|\mathbf{s} - \hat{\mathbf{s}}\|^2\} = \sigma^2 \text{tr}\{\overline{\mathbf{F}}(\widetilde{\mathbf{F}}^T\widetilde{\mathbf{F}})^{-1}\overline{\mathbf{F}}^T\}.$$

If  $\widetilde{\mathbf{F}}$  does not have full rank, perfect signal recovery cannot be guaranteed. Nonetheless, we can still use its pseudo-inverse

(computed via an SVD) to compute the signal and coefficient estimates in (4); alternatively, we can use a Tikhonov regularization ( $\ell_2$  penalty on the norm of  $\hat{\xi}$ ) to obtain the regularized coefficient estimate

$$\hat{\xi} = (\tilde{\mathbf{F}}^T \tilde{\mathbf{F}} + \lambda \mathbf{I})^{-1} \tilde{\mathbf{F}}^T \mathbf{x}.$$

The same estimator can be used in the case of noisy measurements. More specifically, assuming that the noise samples  $v[n]$ ,  $n \in \mathcal{M}$ , are uncorrelated with known average power  $\sigma^2$ , and the coefficients  $\xi_{kl}$  are uncorrelated with average power  $P^2$ , we choose  $\lambda = \sigma^2/P^2$ .

Since our signal model uses sparse basis vectors (i.e., with small support), even if  $\tilde{\mathbf{F}}$  doesn't have full rank (typically because the sampling density is too low in certain parts of the graph), the reconstruction errors will remain localized within that region, i.e., the reconstruction in the remainder of the graph will still be accurate (see Section IV). This is an important advantage of our LGFF model.

### B. Computational Aspects

In practice, rather than inverting the Gramian of  $\tilde{\mathbf{F}}$ , it is preferable to compute the coefficients  $\hat{\xi}$  by solving the normal equations

$$\tilde{\mathbf{F}}^T \tilde{\mathbf{F}} \hat{\xi} = \tilde{\mathbf{F}}^T \mathbf{x} \quad (5)$$

(or their regularized version) and exploit the fact that  $\tilde{\mathbf{F}}$  is usually sparse. With  $\mathcal{M}_k = \mathcal{S}_k \cap \mathcal{M}$  denoting the sampled vertices within  $\mathcal{S}_k$ , the number of nonzero elements of a column  $\tilde{\mathbf{f}}_{kl} = \mathbf{M} \mathbf{f}_{kl}$  of  $\tilde{\mathbf{F}}$  equals at most  $M_k = |\mathcal{M}_k|$ . Hence, the total number of nonzero elements in  $\tilde{\mathbf{F}}$  is  $B_0 \sum_{k=1}^K M_k \geq MB/K$ , typically entailing a sparsity level of  $\mathcal{O}(1/K)$ .

The gradient descent iterations for (5) with step size  $\alpha$  read

$$\hat{\xi}_{i+1} = \hat{\xi}_i - \alpha \tilde{\mathbf{F}}^T \mathbf{r}_i \quad \text{with } \mathbf{r}_i = \tilde{\mathbf{F}} \hat{\xi}_i - \mathbf{x},$$

and hence consist of simple and cheap alternating multiplications with  $\tilde{\mathbf{F}}$  and  $\tilde{\mathbf{F}}^T$ . For the regularized problem, the previous estimate  $\hat{\xi}_i$  in the update is dampened by a factor of  $(1 - \alpha\lambda)$ .

Multiplication with  $\tilde{\mathbf{F}}^T$  basically amounts to aggregating the values within  $\mathcal{S}_k$ ,

$$\sum_{n \in \mathcal{M}_k} f_{kl}[n] r_i[n].$$

Multiplication with  $\tilde{\mathbf{F}}$  by contrast results in signal synthesis on the sampling locations. Since the basis functions have limited overlap, we only need to super-impose the ones with non-zero support at any given location, i.e., with  $\mathcal{K}(n) = \{k: n \in \mathcal{S}_k\}$

$$\sum_{k \in \mathcal{K}(n)} \sum_{l=1}^{B_0} f_{kl}[n] \hat{\xi}_{kl}^{(i)}, \quad n \in \mathcal{M},$$

Similar remarks apply when more advanced solvers (e.g., LSQR [26]) are used to solve the normal equations. We finally note that once the coefficient estimates are obtained, the graph signal reconstruction according to (2) can be done similarly efficiently with complexity  $\mathcal{O}(\eta NB/K)$ . Hence, our methods are typically  $K$  times faster than for non-sparse signal models.

### C. Special Cases

We discuss a few special cases to highlight some advantages of our model and methods.

*Non-overlapping windows.* First consider the orthogonal LGFF with windows that equal the indicator functions of  $\mathcal{S}_k = \mathcal{V}_k$ ,  $\mathbf{g}_k = \chi_k$ , and hence are non-overlapping,  $\mathbf{g}_k \odot \mathbf{g}_{k'} = \mathbf{0}$  for  $k' \neq k$ . This entails that the frame vectors belonging to different subgraphs have disjoint support and hence  $\tilde{\mathbf{F}}$  and  $\tilde{\mathbf{F}}$  (with appropriate vertex permutations) feature a block structure, with the blocks having dimension  $M_k \times B_0$ . As a result, the normal equations (5) decouple into  $K$  separate equations (with  $M_k$  observations and  $B_0$  unknowns each) and can be solved for each subgraph independently. Since  $g_k[n] = 1$  for  $n \in \mathcal{S}_k$ , the  $M_k \times B_0$  sampled basis matrix within  $\mathcal{S}_k$  reads  $\tilde{\mathbf{F}}_k = \mathbf{M} \mathbf{S}_k(\mathbf{u}_{k1} \dots \mathbf{u}_{kB_0})$ . In order for  $\tilde{\mathbf{F}}_k$  to have full rank (necessary for perfect reconstruction), we need  $M_k \geq B_0$  and sampling locations  $\mathcal{M}_k$  that preserve the linear independence of the (orthonormal) local Fourier basis vectors  $\mathbf{u}_{kl}$ ,  $l = 1, \dots, B_0$ . This is usually easier to achieve for local Fourier bases with small coherence (cf. [10]).

*Separating sampling sets.* Even if the windows  $\mathbf{g}_k$  feature a roll-off and overlap, the overlap doesn't necessarily affect all vertices. The set of nodes  $\mathcal{S}'_k \subseteq \mathcal{S}_k$  within subgraph  $\mathcal{G}_k$  that are unaffected by the overlap are given by

$$\mathcal{S}'_k = \overline{\bigcup_{i \neq k} \mathcal{S}_i},$$

where  $\bar{\mathcal{S}} = \mathcal{V} \setminus \mathcal{S}$  denotes the vertex complement. If  $\mathcal{M}_k \subseteq \mathcal{S}'_k$ ,  $k = 1, \dots, K$ , i.e., all sample locations lie within the non-overlap regions, we call  $\mathcal{M}$  a separating sampling set and conclude that the reconstruction can again be computed locally by solving  $K$  smaller problems within each subgraph. Since  $g_k[n] = 1$  for  $n \in \mathcal{S}'_k$ , the discussion regarding the sampled basis matrix for non-overlapping windows here applies as well.

*Case  $B_0 = 1$ .* Here, we have  $B = K$  unknown LGFF coefficients. Since  $\mathbf{u}_{k1} = 1/\sqrt{N_k}$ , the sampled LGFS basis is given by  $\tilde{\mathbf{F}} = (\tilde{\mathbf{g}}_1 \dots \tilde{\mathbf{g}}_K)$ , with  $\tilde{\mathbf{g}}_k = \mathbf{M} \mathbf{g}_k / \sqrt{N_k}$ , i.e., the elements of the sampled basis are  $(\tilde{\mathbf{F}})_{mk} = g_k[n_m] / \sqrt{N_k}$ . With constant windows or separating sample sets, we further have  $g_k[n_m] = 1$  for  $n_m \in \mathcal{M}_k$  and  $g_k[n_m] = 0$  else. It follows that  $\tilde{\mathbf{F}}^T \tilde{\mathbf{F}} = \text{Diag}(M_1/N_1, \dots, M_K/N_K)$  and hence  $\hat{\xi}_k = \frac{\sqrt{N_k}}{M_k} \sum_{n \in \mathcal{M}_k} x[n]$  and  $\hat{s}[n] = g_k[n] \hat{\xi}_k / \sqrt{N_k}$  for  $n \in \mathcal{S}_k$ .

*Regular graphs.* Consider a connected 2-regular graph (cycle) or the 4-regular grid graph obtained as Cartesian product of two cycle graphs. When these graphs are partitioned into contiguous subgraphs of equal size, our LGFS model becomes a discrete equivalent of shift-invariant spaces, for which sampling has been extensively studied [27].

## IV. EXPERIMENTS

We next illustrate the performance of our method via numerical simulations. We first show an exemplary reconstruction on a random geometric graph with  $N = 2048$  nodes. The graph signal (shown in Fig. 1(a)) lies in an LGFS with  $K = 128$

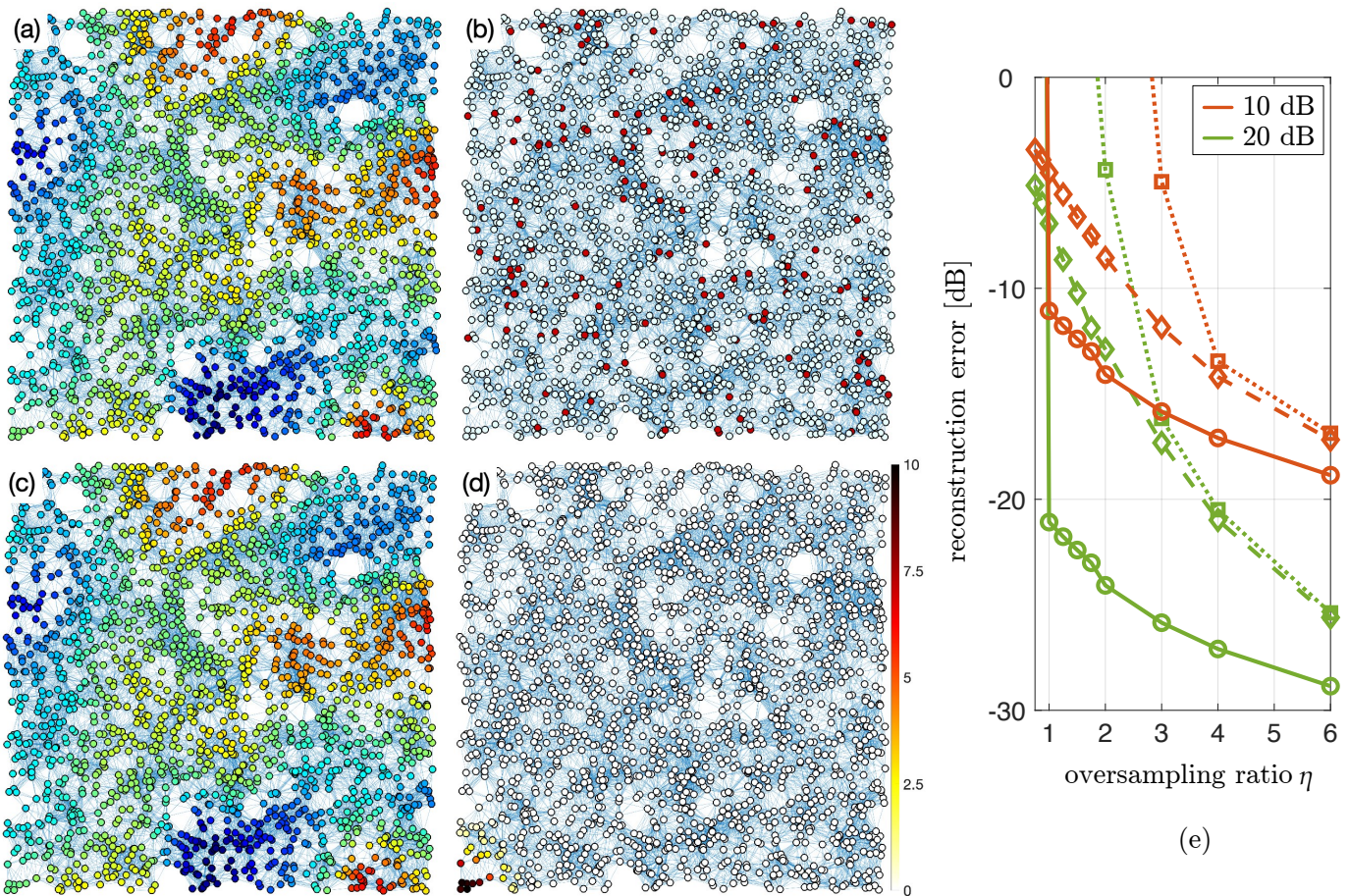


Fig. 1. Illustrative reconstruction example: (a) an LGFS signal (color indicates signal value) with  $K = 128$ ,  $B_0 = 1$ , and  $I = 3$  on a random geometric graph with  $N = 2048$  nodes; (b) red vertices indicate  $M = 160$  sampling locations (rank of  $\tilde{\mathbf{F}}$  is 125); (c) reconstructed graph signal (normalized reconstruction error  $-43.5$  dB); (d) reconstruction error (in percent of average signal strength). (e) The average reconstruction error achieved with separating sampling sets ( $\text{---}\circ\text{---}$ ), random sampling sets ( $\text{---}\square\text{---}$ ), and random sampling sets with regularized interpolation ( $\text{---}\diamond\text{---}$ ) at noise levels of 10 and 20 dB versus oversampling ratio (signals from an LGFS with  $K = 8$ ,  $B_0 = 1$ , and  $I = 1$  on a random geometric graph with  $N = 1024$  nodes).

subgraphs, local bandwidth  $B_0 = 1$ , and roll-off  $I = 3$ . We use a randomly drawn sampling set consisting of  $M = 160$  vertices (oversampling ratio  $\eta = 1.25$ , see Fig. 1(b)), which led to a  $160 \times 128$  sampled basis matrix  $\tilde{\mathbf{F}}$  of rank 125. Due to the rank-deficiency, perfect recovery is not possible. Surprisingly, least-squares reconstruction yields an LGFS signal (Fig. 1(c)) with a normalized reconstruction error of  $-43.5$  dB. Even more astonishing is the fact that the reconstruction error is highly localized in the region of the graph where there are insufficient sampling locations (cf. the lower left corner of Fig. 1(d)), thus only affecting no more than 2% of the nodes.

For a more systematic performance investigation, we next consider random geometric graphs with  $N = 1024$  nodes and LGFS with  $K = 8$  subgraphs, local bandwidth  $B_0 = 1$ , and roll-off  $I = 1$ . We performed signal reconstruction at signal-to-noise ratios of 10 dB and 20 dB and oversampling ratios  $\eta \in [1, 6]$  based on random sampling sets (with and without regularization) and on separating sampling sets. The normalized reconstruction error, averaged over 300 graph realizations and 1000 signal realizations, is shown in Fig. 1(e). It is seen that reconstruction performance improves with increasing sam-

pling rate. Separating sampling sets systematically outperform random sampling sets by a substantial margin and essentially work even for critical sampling. By contrast, random sampling tends to require larger sampling rates to achieve comparable performance, specifically without regularization. We note that bandlimited GFT-based reconstruction typically performed 10-20 dB worse despite substantially higher computational complexity (results not depicted).

## V. CONCLUSION

We have discussed simple vertex-domain sampling and reconstruction methods for a sparse signal model that is based on local graph Fourier frames (LGFFs). We have found that separating sampling sets facilitate perfect reconstruction but even randomly chosen sampling sets result in accurate signal recovery. The two main advantages of our approach are its computational efficiency and the containment of reconstruction errors to regions of the graph where the sampling density is too small. In our future work we plan to analyze the probability for successful recovery with random sampling sets using tools from compressive sensing in the style of [10].

## REFERENCES

- [1] A. Ortega, *Introduction to Graph Signal Processing*, 1st ed. Cambridge, UK: Cambridge Univ. Press, Jun. 2022.
- [2] L. Stanković, D. Mandić, M. Daković, M. Brajović, B. Scalzo, S. Li, and A. G. Constantinides, "Data Analytics on Graphs, Parts I-III," *Foundations and Trends in Machine Learning*, vol. 13, no. 4, pp. 1–530, 2020.
- [3] P. M. Djurić and C. Richard, Eds., *Cooperative and Graph Signal Processing*. Academic Press, 2018.
- [4] Y. Tanaka, Y. C. Eldar, A. Ortega, and G. Cheung, "Sampling signals on graphs: From theory to applications," *IEEE Signal Process. Mag.*, vol. 37, no. 6, pp. 14–30, Nov. 2020.
- [5] I. Pesenson, "Sampling in Paley-Wiener spaces on combinatorial graphs," *Trans. Am. Math. Soc.*, vol. 361, no. 7, Nov. 2011.
- [6] A. Gadde and A. Ortega, "A probabilistic interpretation of sampling theory of graph signals," in *Proc. Int. Conf. Acoust., Speech, and Signal Proc.*, Brisbane, Australia, Apr. 2015, pp. 3257–3261.
- [7] A. Anis, A. Gadde, and A. Ortega, "Efficient sampling set selection for bandlimited graph signals using graph spectral proxies," *IEEE Trans. Signal Process.*, vol. 64, no. 14, pp. 3775–3789, July 2016.
- [8] M. Tsitsvero, S. Barbarossa, and P. Di Lorenzo, "Signals on graphs: uncertainty principle and sampling," *IEEE Trans. Signal Process.*, vol. 64, no. 18, pp. 4845–4860, Sept. 2016.
- [9] S. Chen, S. Varma, A. Sandryhaila, and J. Kovačević, "Discrete signal processing on graphs: Sampling theory," *IEEE Trans. Signal Process.*, vol. 63, no. 24, pp. 6510–6523, Dec. 2015.
- [10] G. Puy, N. Tremblay, R. Gribonval, and P. Vandergheynst, "Random sampling of bandlimited signals on graphs," *Applied and Computational Harmonic Analysis*, vol. 44, no. 2, pp. 446–475, March 2018.
- [11] A. G. Marques, S. Segarra, G. Leus, and A. Ribeiro, "Sampling of graph signals with successive local aggregations," *IEEE Trans. Signal Process.*, vol. 64, no. 7, pp. 1832–1843, Apr. 2016.
- [12] M. Belkin, I. Matveeva, and P. Niyogi, "Regularization and semi-supervised learning on large graphs," in *Proc. Annual Conf. Learning Theory (COLT)*, Banff, Canada, July 2004, pp. 624–638.
- [13] G. Hannak, P. Berger, A. Jung, and G. Matz, "Efficient graph signal recovery over big networks," in *Proc. Asilomar Conf. Signals, Systems, Computers*, Pacific Grove, CA, Nov. 2016, pp. 1839–1843.
- [14] P. Berger, G. Hannak, and G. Matz, "Graph signal recovery via primal-dual algorithms for total variation minimization," *IEEE Journal of Selected Topics in Signal Processing*, vol. 11, no. 6, pp. 842–855, Sept. 2017.
- [15] P. Reingruber and G. Matz, "Tight local graph Fourier frames with finite support," in *Proc. Asilomar Conf. Signals, Systems and Computers*, Pacific Grove, CA, Oct. 2024.
- [16] D. K. Hammond, P. Vandergheynst, and R. Gribonval, "Wavelets on graphs via spectral graph theory," *Appl. Comput. Harmon. Anal.*, vol. 30, no. 2, pp. 129–150, Mar. 2011.
- [17] B. de Loynes, F. Navarro, and B. Olivier, "Localized Fourier analysis for graph signal processing," *Appl. Comput. Harmon. Anal.*, vol. 57, pp. 1–26, Mar. 2022.
- [18] H. Behjat, U. Richter, D. Van De Ville, and L. Sornmo, "Signal-Adapted Tight Frames on Graphs," *IEEE Trans. Signal Process.*, vol. 64, no. 22, pp. 6017–6029, Nov. 2016.
- [19] D. I. Shuman, C. Wiesmeyer, N. Holighaus, and P. Vandergheynst, "Spectrum-Adapted Tight Graph Wavelet and Vertex-Frequency Frames," *IEEE Trans. Signal Process.*, vol. 63, no. 16, pp. 4223–4235, Aug. 2015.
- [20] F. Göbel, G. Blanchard, and U. V. Luxburg, "Construction of Tight Frames on Graphs and Application to Denoising," in *Handbook of Big Data Analytics*, ser. Springer Handbooks of Computational Statistics, W. K. Härdle, H. H.-S. Lu, and X. Shen, Eds. Cham, Switzerland: Springer, 2018, pp. 503–522.
- [21] N. Tremblay and P. Borgnat, "Subgraph-Based Filterbanks for Graph Signals," *IEEE Trans. Signal Process.*, vol. 64, no. 15, pp. 3827–3840, Aug. 2016.
- [22] M. Coutino, S. P. Chepuri, T. Maehara, and G. Leus, "Fast Spectral Approximation of Structured Graphs with Applications to Graph Filtering," *Algorithms*, vol. 13, no. 9, p. 214, Aug. 2020.
- [23] O. Christensen, *An Introduction to Frames and Riesz Bases*, ser. Applied and Numerical Harmonic Analysis. Boston, MA, USA: Birkhäuser, 2016.
- [24] R. R. Coifman and Y. Meyer, "Remarques sur l'analyse de Fourier à fenêtre," *C. R. Acad. Sci.*, vol. 312, no. 1, pp. 259–261, 1991.
- [25] H. S. Malvar, "Lapped transforms for efficient transform/subband coding," *IEEE Trans. Acoust., Speech, Signal Process.*, vol. 38, pp. 969–978, Jun. 1990.
- [26] C. C. Paige and M. A. Saunders, "LSQR: an algorithm for sparse linear equations and sparse least squares," *ACM Trans. Math. Software*, vol. 8, no. 1, pp. 43–71, June 1982.
- [27] A. Aldroubi and K. Gröchenig, "Nonuniform sampling and reconstruction in shift-invariant spaces," *SIAM Review*, vol. 43, no. 4, pp. 585–620, 2001.